

Design of a low-cost, high-precision rolling nanoelectrode lithography machine for manufacturing nanoscale products

Zhengjian Wang¹, Xichun Luo^{*1}, Rashed Md. Murad Hasan¹, Wenkun Xie¹, Wenlong Chang², Qi Liu¹

¹ Centre for Precision Manufacturing, DMEM, University of Strathclyde, United Kingdom

² Innova Nanojet Technologies Ltd., Glasgow G1 1RD, United Kingdom

zhengjian.wang@strath.ac.uk

Abstract

This paper presents the design of a low-cost, high-precision rolling nanoelectrode lithography (RNEL) machine, addressing the growing demand for cost-effective and high-precision nanomanufacturing processes for next-generation nanoproducts. Unlike plate-to-plate methods, the rolling stamp ensures uniform contact pressure across the entire surface of the 8-inch substrates, simplifying the separation process. However, achieving precise positioning between the rolling stamp and substrate during RNEL operations is essential, as even slight deviations can lead to significant defects in fabricated nanostructures. This poses a considerable challenge in developing an affordable, high-precision RNEL machine that meets the requirements for high-yield production, especially for SMEs. The final design adopts a four-axis fixed-gantry configuration where the X- and Y-axes are mounted separately, chosen from four candidates for the superior overall performance. The machine employs a step-and-repeat mechanism using three low-cost ball-bearing linear slides. Additionally, a flexure-based passive tilting stage with nanometre resolution is integrated into the roller unit, promoting high alignment accuracy and uniform contact. In simulations, a 5 N load at the rolling stamp's edge causes a rotation of about 0.00022 radians with only a tiny lateral deformation of 4.9 nm. While the current design achieves an RSS error of approximately 10 μm , attaining the desired sub-micron positioning accuracy requires further developments, particularly in compensating for geometric and thermal errors. Addressing these issues is the next step in our research, aiming to fulfil the precision demands of RNEL operations.

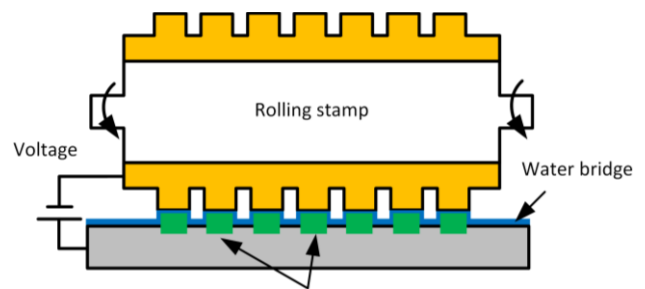
Keywords: Rolling nanoelectrode; Lithography machine; Flexure tilting stage

1. Introduction

The demand for next-generation nanoscale products, such as photonic integrated circuits and heat-assisted magnetic recording disks, is rapidly increasing. These products require high-precision nanostructures with diverse functionalities to meet varied user needs. Consequently, there is a growing need for low-cost, high-precision nanomanufacturing processes and machines, especially for rapid prototyping to reduce time-to-market.

Rolling Nanoelectrode Lithography (RNEL), a recent innovation from the University of Strathclyde, offers a promising solution in nanofabrication [1]. This technique leverages anodic oxidation confined spatially between a conductive rolling stamp and the substrate surface to create nanostructures (see Figure 1). RNEL offers high production efficiency and great flexibility in manufacturing various nanostructures by controlling processing parameters, such as applied voltage, rolling speed, and humidity, without changing stamps [2].

In this context, this paper aims to design a low-cost, high-precision RNEL machine. This design incorporates a rolling stamp, ensuring uniform contact pressure across the substrate, which simplifies the separation process. Even minor misalignments can lead to significant defects in the resulting nanostructures, presenting considerable challenges in developing an affordable, high-precision RNEL machine suitable for high-yield production at costs feasible for SMEs. These issues will be considered in the design process, which is the focus of this paper.



Fabricated nanoscale structures
Figure 1. Working principle of RNEL

In this paper, Section 2 introduces the selection process for the RNEL machine's configuration, including analyses of the error budget, static and dynamic characteristics to assess maximum geometric errors, thermal sensitivity and vibrational modes. Section 3 presents the design of a flexure-based passive tilting stage, aiming to enable precise alignment and uniform contact distribution between the rolling stamp and substrate.

2. Machine configuration and performance analysis

The materials of the substrate are silicon or silicon carbide; the maximum size of the workpiece is 8 inches (approximately 200 mm) in diameter. Table 1 displays the specifications of the RNEL machine, which are designed based on the substrate specifications. A four-axis configuration was chosen, utilising three low-cost ball-bearing slides as the X-, Y-, and Z-axes to move the rolling stamp toward the substrate. The rolling stamp's effective length was designed to be 90 mm, which is

nearly half the diameter of the 8-inch substrate, reducing manufacturing difficulties and costs associated with the rolling stamps. The proposed RNEL machine performs the step-and-repeat action to generate nanostructures on the 8-inch wafers. The proposed RNEL machine employs the step-and-repeat

action to generate nanostructures on the 8-inch wafers. To achieve nanometer-level motion accuracy, a novel air-bearing rolling stamp unit was designed to hold and rotate the rolling stamp.

Table 1. Specifications of the RNEL machine

Axis number	Type	Stroke	Drive system	Motion accuracy	Resolution
X-axis	Ball-bearing	250 mm	Linear motor	<2 μm	5 nm
Y-axis	Ball-bearing	200 mm	Linear motor	<2 μm	5 nm
Z-axis	Ball-bearing	60 mm	Linear motor	<0.5 μm	1 nm
B-axis	Air-bearing	360°	Direct drive torque motor	<2 arcsec	0.02 arcsec

Four roll-to-plate machine configurations were proposed during the conceptual design stage, as shown in Figure 2.

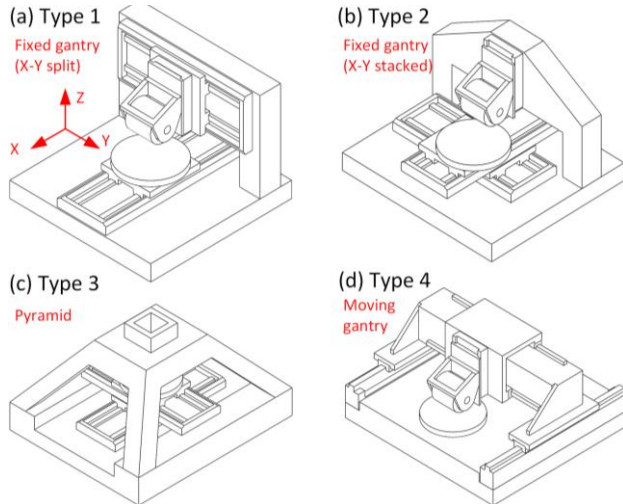


Figure 2. Four candidate configurations of the RNEL machine: (a) Type 1; (b) Type 2; (c) Type 3; (d) Type 4

The error budget estimates potential errors within a machine axis, resulting in deviations from the intended motion. It is utilised as a method for evaluating the capacity of a proposed machine configuration to fulfil the desired specifications [3]. It is an effective tool for predicting the geometric error of a machine system. Figure 3 and Figure 4 illustrate the error budget of Type 1 and Type 4 machine configurations, respectively.

Axis	Feature	Value	Abbe offset	Error (μm)		
X	Pitch	9.3 arcsec	45 mm	2.03	2.03	4.51
	Yaw	9.3 arcsec	100 mm	4.51		
	Roll (Y)	9.3 arcsec	45 mm			
	Roll (Z)	9.3 arcsec	100 mm			
	Straightness	$\pm 3 \mu\text{m}$		6.00		
	Flatness	$\pm 3 \mu\text{m}$		6.00		
Y	Pitch	8.2 arcsec	130 mm	5.17	5.17	4.37
	Yaw	8.2 arcsec	110 mm	4.37		
	Roll (X)	8.2 arcsec	130 mm			
	Roll (Z)	8.2 arcsec	110 mm			
	Straightness	$\pm 2.5 \mu\text{m}$		5.00		
	Flatness	$\pm 2.5 \mu\text{m}$		5.00		
Z	Pitch	10 arcsec	59 mm	3.27	2.86	2.86
	Yaw	5 arcsec	135 mm	2.06		
	Roll (X)	10 arcsec	42.5 mm			
	Roll (Y)	10 arcsec	59 mm			
	Straightness	$\pm 1.5 \mu\text{m}$		3.00		
	Flatness	$\pm 1.5 \mu\text{m}$		3.00		
B	Radial error (X)	1 μm		1.00	1.00	1.00
	Axial error (Y)	1 μm		1.00		
	Radial error (Z)	1 μm				
	Tilt error (X)	2 arcsec	42.5 mm	0.41		
	Tilt error (Y)	2 arcsec	45 mm	0.44		
Total error				23.18	28.14	23.74
RSS error				9.52	10.73	10.47

Figure 3. Error budget of Type 1 machine configuration

Axis	Feature	Value	Abbe offset	Error (μm)		
X	Pitch	15 arcsec	20 mm	1.45	3.64	7.82
	Yaw	15 arcsec	42.5 mm	3.09		
	Roll (Y)	15 arcsec	50 mm			
	Roll (Z)	15 arcsec	107.5 mm			
	Straightness	$\pm 3 \mu\text{m}$		6.00		
	Flatness	$\pm 3 \mu\text{m}$		6.00		
Y	Pitch	15 arcsec	110 mm	8.00	8.00	13.45
	Yaw	15 arcsec	185 mm			
	Roll (X)	15 arcsec	110 mm			
	Roll (Z)	15 arcsec	185 mm			
	Straightness	$\pm 3 \mu\text{m}$		6.00		
	Flatness	$\pm 3 \mu\text{m}$		6.00		
Z	Pitch	10 arcsec	75 mm	2.06	3.64	3.64
	Yaw	5 arcsec	150 mm			
	Roll (X)	10 arcsec	42.5 mm			
	Roll (Y)	10 arcsec	75 mm			
	Straightness	$\pm 1.5 \mu\text{m}$		3.00		
	Flatness	$\pm 1.5 \mu\text{m}$		3.00		
B	Radial error (X)	1 μm		1.00	1.00	1.00
	Axial error (Y)	1 μm		1.00		
	Radial error (Z)	1 μm				
	Tilt error (X)	2 arcsec	42.5 mm	0.41		
	Tilt error (Y)	2 arcsec	45 mm	0.44		
Total error				25.02	42.80	37.91
RSS error				11.23	18.19	18.12

Figure 4. Error budget of Type 4 machine configuration

Following the same fashion, the root sum square (RSS) error of Type 2 and Type 3 configurations is obtained and presented in Table 2.

Table 2. RSS error of Type 2 and 3 configurations

Configuration	RSS error (X)	RSS error (Y)	RSS error (Z)
Type 2	9.52	11.31	11.73
Type 3	9.35	11.21	11.52

Figure 3 reveals that the RSS error of Type 1 configuration in each direction is approximately 10 μm . This suggests that geometric error compensation is necessary for nanomanufacturing manipulation, a task that will be addressed in future work by the authors.

It's worth mentioning that the first three configurations exhibit minimal error differences due to the similarity in specifications and the dimensions of the components. Type 4 configuration has the largest RSS error because of the low-stiffness nature of the moving gantry.

The modal analysis is conducted to assess the dynamic performance of the proposed configurations, and the results are presented in Figure 4. Spring-damper elements were employed to model the dynamic behaviour of the ball bearings.

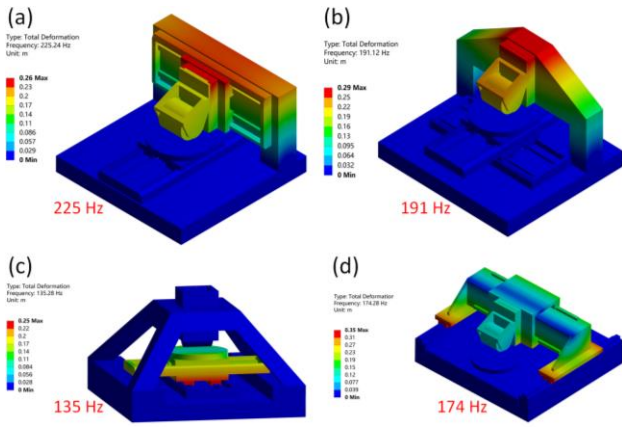


Figure 5. Dynamic performance analysis

The simulation results indicate that the pyramid type exhibits the worst dynamic performance at 135 Hz, whereas the fixed gantry with an X- and Y-axis split design (Type 1) demonstrates the best dynamic performance at 225 Hz.

Since the roller unit operates at extremely low rotation speeds, a large amount of heat is generated during its operation. Therefore, thermal performance analysis is essential to enhance the machine's efficiency, durability, and overall reliability for every candidate configuration. The thermal sensitivity of each configuration is assessed. The performance indicator is the deformation between the rolling stamp and the substrate as the ambient air temperature increases from 20 to 21 °C. The results are illustrated in Figure 6.

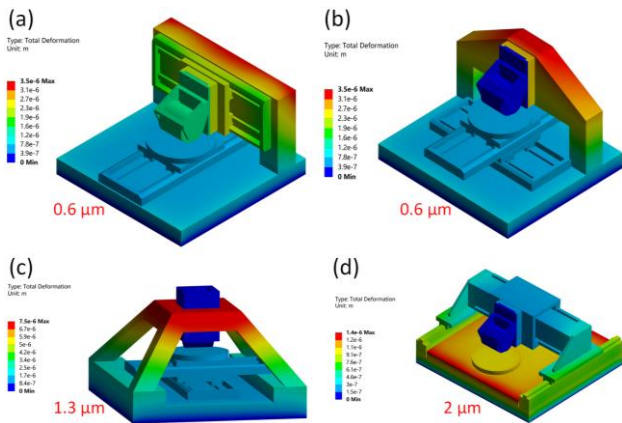


Figure 6. Dynamic performance analysis

It can be concluded that the moving-gantry type is the most vulnerable configuration to temperature fluctuation, with thermal deformation reaching up to 2 μm. In contrast, the fixed gantry type is less sensitive to thermal variation, exhibiting a deformation of only 0.6 μm.

Ultimately, when summarising the results of all performance analyses, it is determined that Type 1 is the best machine configuration, so it was adopted as the configuration for the proposed machine.

3. Flexure-based passive tilting stage

The seamless and uniform contact between the rolling stamp and substrate is a prerequisite for manufacturing consistent nanostructures with high resolution. For instance, there may be an angular misalignment α (see Figure 7) between the template and substrate when they are not parallel.

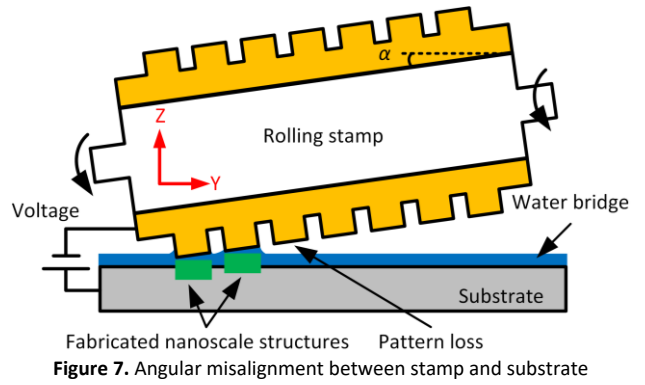


Figure 7. Angular misalignment between stamp and substrate

An excessive misalignment will prevent the electrochemical reaction from occurring uniformly across the entire touched area, leading to pattern loss. An angle compensation remains far from the success of high-accuracy nanopatterning. This is because when the rotation axis of the tilting motion is not on the surface of the stamp, the coupled lateral displacement will increase the overlay error [4, 5]. A four-bar flexure-based tilting stage with semi-circular notches will be introduced to hold the rolling stamp with an angle compensation mechanism to address the above issues. Also, the centre of rotation was designed to coincide with the centre of the rolling stamp's outer edge to control its lateral displacement and prevent slippage between the stamp and substrate.

The semi-circular notches were designed so that when a 5 N load is applied to the edge of the rolling stamp, the roller rotates about 0.00025 radians. After sufficient calculations, the key dimensional parameters of the semi-circular notches, denoted as b , L , R , and t (as illustrated in Figure 8), were confirmed as 20 mm, 20 mm, 3.7 mm, and 0.4 mm, respectively. The material chosen for manufacturing the notches is 7075 aluminium alloy.

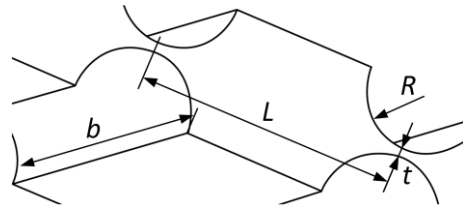


Figure 8. Semi-circular notches

The static analysis was then conducted to evaluate the tilting performance, and the results are shown in Figure 9. A deformation in the Z-direction of about 10 μm can be observed on both sides of the rolling stamp, indicating a rotation angle of 0.00022 radians. Most importantly, as illustrated in Figure 9(b), the rolling stamp moves laterally by only 4.9 nm, demonstrating excellent alignment accuracy.

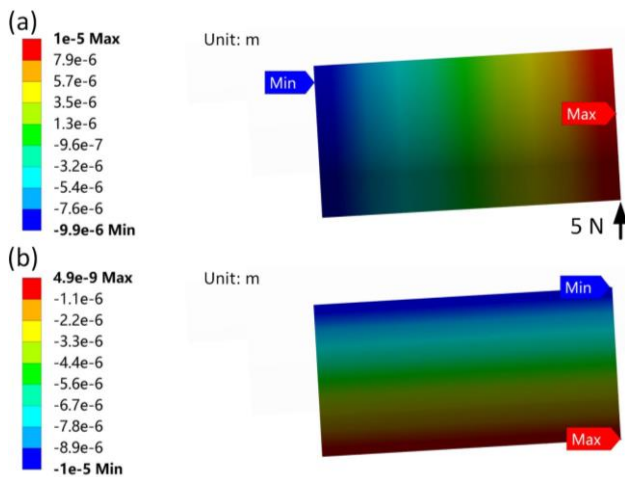


Figure 9. (a) Simulated tilting deformation under an external force of 5 N; (b) simulated lateral deformation.

4. Conclusion

This study presents the design of a low-cost, high-precision rolling nanoelectrode lithography (RNEL) machine. After thoroughly evaluating four machine configuration candidates, the selected configuration emerged as remarkable, excelling in dynamic and thermal performance while minimising geometric errors. A key feature of our design is the incorporation of a flexure-based passive tilting stage within the roller unit, achieving high alignment accuracy and ensuring consistent contact between the rolling stamp and substrate. Simulation results demonstrate that under a 5 N load applied at the edge of the rolling stamp, the roller rotates about 0.00022 radians with a minimal lateral deformation of 4.9 nm. However, the integration of cost-effective ball-bearing linear stages resulted in an RSS error of approximately 10 μm in each direction. This deviation is significant for RNEL operations. The next phase of our research will involve the development and implementation of advanced geometric and thermal error compensation techniques to bridge the gap between the current capabilities and the desired sub-micron positioning accuracy.

References

- [1] Hasan R M M, Luo X and Sun J 2020 *Micromachines* **11** 656
- [2] Hasan R M M, Politano O and Luo X 2019 *Appl. Surf. Sci.* **496** 143679
- [3] Chen W, Luo X, Su H and Wardle F 2016 *Int. J. Adv. Manuf. Technol.* **84** 1177
- [4] Lim H, Jung S, Ahn J, Choi K B, Kim G, Kwon S and Lee J 2020 *Materials (Basel)* **13** 1938
- [5] Choi B J, Sreenivasan S V, Johnson S, Colburn M and Wilson C G, 2001 *Precis. Eng.* **25** 192